The Physicochemical Causes of Baseline Disturbances in HPLC, Part I – TFA-Containing Eluents

K. Choikhet, B. Glatz and G. Rozing,
Agilent Technologies Deutschland GmbH, Waldbronn, Germany.

A systematic investigation of the ubiquitous baseline disturbances in reversed-phase liquid chromatographic methods, where UV-absorbing mobile-phase modifiers or additives such as trifluoroacetic acid are used, has been conducted. Problem verification and investigation of possible causes are described. A quantitative model explaining the observations and experiments that validate this model are given and recommendations for the practical use of such additives are presented.

Introduction

Since the introduction of trifluoroacetic acid (TFA) as a mobile phase additive in the reversed-phase (RP) HPLC separation of peptides and proteins 25 years ago[1] its use has remained popular. TFA forms strong ion-pairs with peptides and proteins and, at the same time, suppresses their interaction with residual silanol groups on the stationary phase reducing potential peak tailing. The combination of these effects has led to the almost universal use of TFA in mobile phases for the gradient elution of peptides from tryptic digests of proteins. The detection wavelength used for such peptide maps is set in the low UV-wavelength range, around 210 nm, because peptides do not generally show strong UV absorption at wavelengths above 230 nm. However, at 210 nm, TFA also has a strong UV-absorption band, which can lead to baseline fluctuations that disturb high-sensitivity measurements.[2] In contrast, these baseline disturbances have been widely used with other strongly UV-absorbing mobile phase modifiers for the purpose of indirect UV detection of ions lacking chromophores.[3] The properties of these additives in chromatographic processes are not anomalous, however, and can be explained by theoretical models.[4–9]

In this article, the manifestation of these baseline fluctuations in an HPLC system is described and a simplified theoretical model[4,5,10] presented that adequately describes them. Experiments confirming the model are presented and recommendations for practical use are given.

Experimental

An 1100 Series HPLC system (Agilent Technologies, Waldbronn, Germany) was used, comprising: solvent degasser, binary pump, autosampler, thermostatted column compartment, diode array detector and a PC with ChemStation software (Agilent Technologies) for control, data acquisition and data handling.

A Jupiter 5 µm C18, 150 × 4.6 mm column (Phenomenex, Torrance, California, USA) was first used in spotting the disturbance phenomena and a Hypersil 5 µm C18, 125 × 4.0 mm column (Thermo Hypersil-Keystone, Runcorn, Cheshire, UK) was used in all other experiments. The capacity factors of acetonitrile (ACN) and TFA were determined in the following manner:

1. k'_{ACN} was determined on the Hypersil column over the range 0–10% (v/v) ACN by isocratic elution at 0.5 mL/min of consecutive ACN concentration steps of 1% (v/v) and recording of the RI effect of a 1 µL ACN injection — solvent A: water; solvent B: 10% (v/v) ACN in water (e.g., $k'_{ACN}(0) = 0.46$; $k'_{ACN}(4) = 0.186$; $k'_{ACN}(10) = 0.110$).
2. k'_{TFA} and β_{TFA} (see Equation 8) were determined as for k'_{ACN} but now recording the TFA-signal at 210 nm of a 0 µL TFA injection from the gas phase. This was achieved by lowering the injector needle into a sample well, with a 20 µL droplet of undiluted TFA at the bottom, and making sure that the needle did not contact the TFA. The amount of TFA absorbed from the vapour phase into the eluent residing

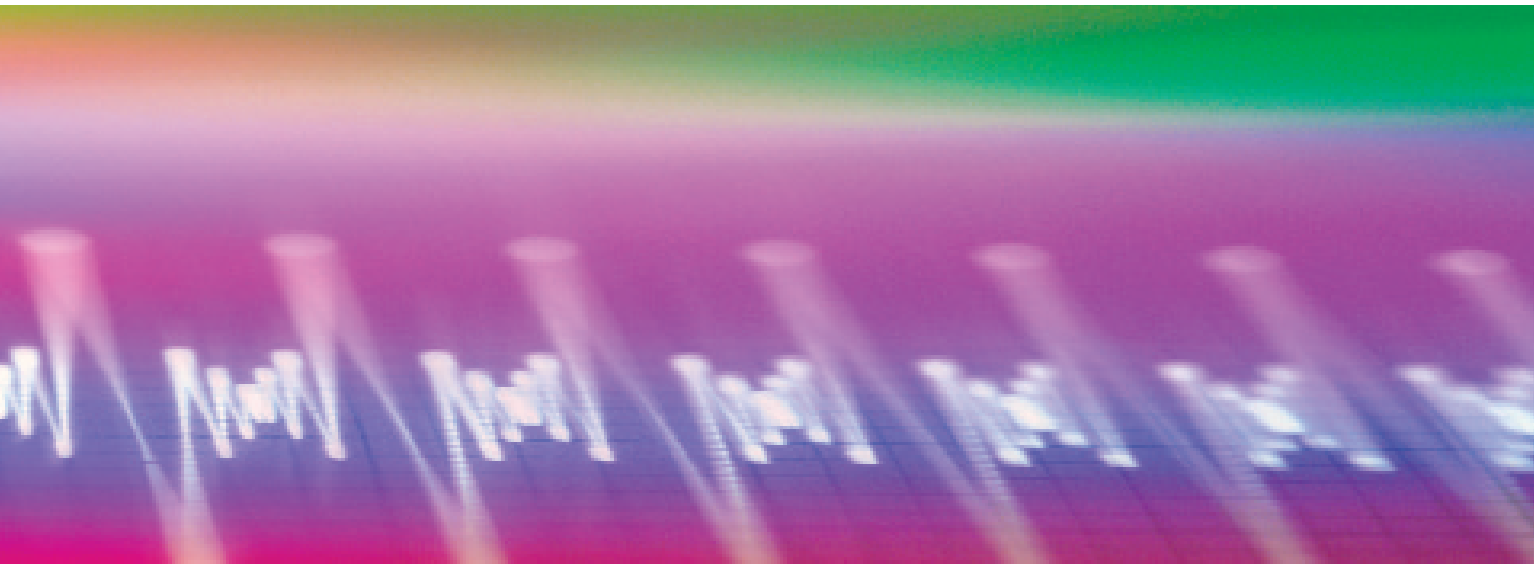

TFA forms strong ion-pairs with peptides and proteins and, at the same time, suppresses their interaction with residual silanol groups on the stationary phase reducing potential peak tailing.

in the needle tip was sufficient as sample — solvent A: water with 0.1% (v/v) TFA; solvent B: 10% (v/v) ACN in water with 0.1% (v/v) TFA (e.g., $k'_{TFA}(0) = 0.338$; $\beta_{TFA} = -0.014$). The column dead time (t_{R0}) was determined by injecting 0 µL of TFA from the gas phase into an isocratic mobile phase of 80% (v/v) ACN in water with 0.1% (v/v) TFA. In the experiments without a column a fused silica restrictor capillary, 960 × 0.1 mm, (Agilent Technologies) was used to simulate the hydrodynamic resistance of the column.

All experiments were performed at 30 °C. All other fractional indications for solutions and eluent compositions in this article are in % (v/v).

TFA and heptafluoric butyric acid (HFBA) were of spectroscopic grade, all other chemicals used were at least analytical or HPLC grade. Chromatograms and spectra were recorded with the diode array detector and ChemStation facilities. Model simulations were performed on a PC with a custom written program in Excel (available on request).

Results and Discussion

Description of the baseline perturbation: In Figure 1, a typical example of the problem is shown. Solvent A is water with 0.1% TFA and solvent B is 80% ACN in water with 0.1% TFA. A gradient of 0–50% solvent B in 50 min was run. At breakthrough of the gradient from the column, the baseline rises in a step and strong fluctuations appear with a periodicity, which correlates to the channel delivering the ACN. The amplitude of the fluctuations decreases with increasing ACN concentration in the solvent mixture.

Verification of the phenomenon: Several factors have been identified that influence the frequency and amplitude of this phenomenon when TFA is used as a mobile-phase additive:

- it occurs with reversed-phase HPLC columns
- it is more pronounced with different types of stationary phase (C18 > C8 > C4 > C1)
- it always correlates with the channel pumping the ACN solvent
- the percentage of ACN in the mobile phase (high disturbances at a low percentage of ACN in the mixture, decreasing with increasing ACN content)
- the pump stroke volume (disturbances decrease with a smaller stroke)
- the concentration of TFA (disturbances increase with a higher concentration)

Figure 1: Baseline perturbations generated with a gradient of 0–50% B in 50 min; solvent A: water with 0.1% TFA, solvent B: 80% ACN in water with 0.1% TFA; detection 210:8 nm, reference 360:100 nm; flow-rate 1.0 mL/min; column: Phenomenex Jupiter 5 µm C18, 150 × 4.6 mm; compressibility settings: pump A: 50, pump B: 115; red trace: pump stroke volume 100 µL, blue trace: pump stroke volume 20 µL.

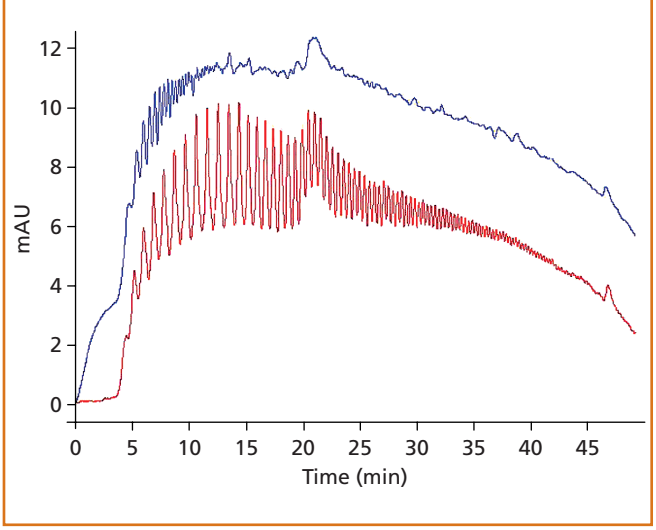

- the detection wavelength (disturbances highly visible at 210 nm, not visible at 250 nm)
- the compressibility settings of pumps (disturbances increase with incorrect settings, especially for the ACN-delivering channel)
- the volume of the mixer (disturbances increase with decreasing volume)
- the performance of pumping valves (disturbances increase with valve leakage)
- insufficient solvent degassing (disturbances increase with higher air content in the solvent).

At the onset of this work, several experiments were performed to confirm and/or expand these field observations.

A concentration of 0.1% TFA in water or ACN causes a relatively high background absorbance of the mobile phase (approximately 550 mAU at 210 nm). When running an isocratic or gradient run with a solvent composition generated from both pump channels, the baseline is set to zero at the beginning of the run. However, this is only a baseline offset compensation. In reality, the baseline remains at a high signal level (~550 mAU) and consequently amplifies TFA concentration fluctuations, which are manifested as visible baseline disturbances. In addition the spectrum of TFA depends on the solvent composition.

To estimate the magnitude of this effect, UV/vis spectra of 0.1% TFA solutions were recorded in solutions ranging from 100% water to 100% ACN. The measurements were performed using a gradient pump for mixing preset solutions of 0.1% TFA in water with either 0.1% TFA in ACN (Figure 2) or water/ACN 1:4 (Figure 3).

As can be seen in Figure 2, the spectra of TFA in up to 75% ACN do not change much with respect to wavelength and height of the absorbance maximum. At higher concentrations of ACN, the absorbance at 210 nm decreases rapidly, while at 220 nm the absorbance increases. All spectra go through a quasi-isosbestic point at 214.5 nm. Therefore, at a detection wavelength of 214 nm minimal baseline drift will result if running a gradient from 0–100% ACN with 0.1% TFA (Figure 3, black trace). Volume contraction on mixing explains the increase of absorbance in the middle region. With the detection wavelength set at 210 nm, the baseline decreases sharply during the 0–100% gradient (Figure 3, green trace) and rises when measured at 220 nm (Figure 3, red trace). This is in accordance with the spectra recorded in Figure 2. It has been reported,[11] that suppression of dissociation and solvochromic effects are the causes for the spectral changes of TFA when the amount of water in the solution is reduced.

Verification of possible causes of baseline perturbations: Without a column installed barely any baseline fluctuations are observed. This is confirmed by the magnified baseline traces in Figure 3. A deliberate illustration of the scope of the problem is given in Figure 4. Here, a binary pump is used to deliver an isocratic mixture of 5% B (80% ACN in water with 0.1% TFA) and 95% A (water with 0.1% TFA).

Figure 2: Spectra of 0.1% TFA in water/ACN mixtures of varying ratios.

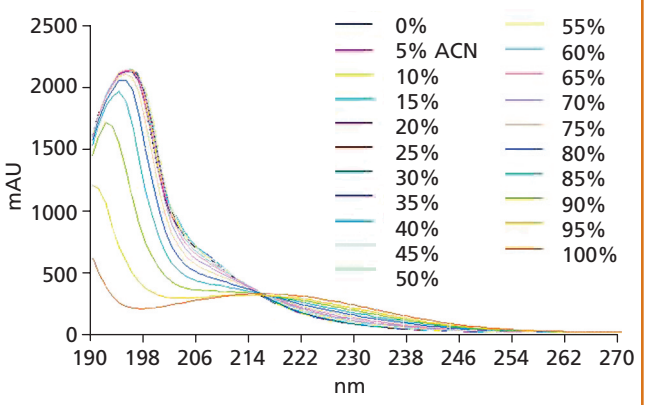

Figure 3: Baseline plots obtained with a gradient of 0–100% B, but without a column, at different wavelengths; solvent A: water with 0.1% TFA, solvent B: 80% ACN in water with 0.1% TFA; flow-rate 1mL/min.

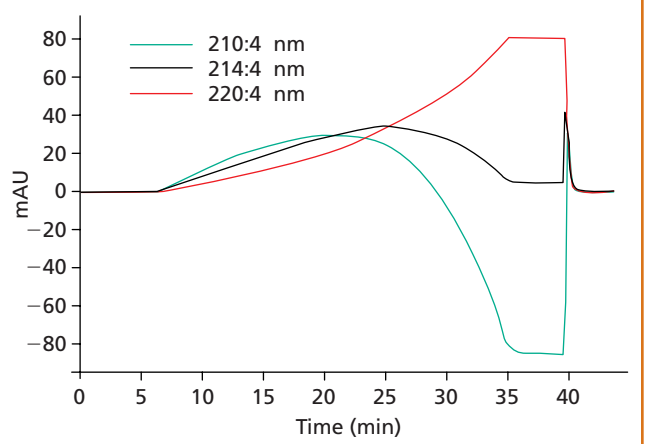

Figure 4: Baseline plots obtained with an isocratic solvent mixture A/B = 95/5, (a) with and (b) without a column, solvents A and B as in Figure 3; column: Hypersil 5 µm C18, 125 × 4.0 mm; detection 210:4 nm; flow-rate 1 mL/min.

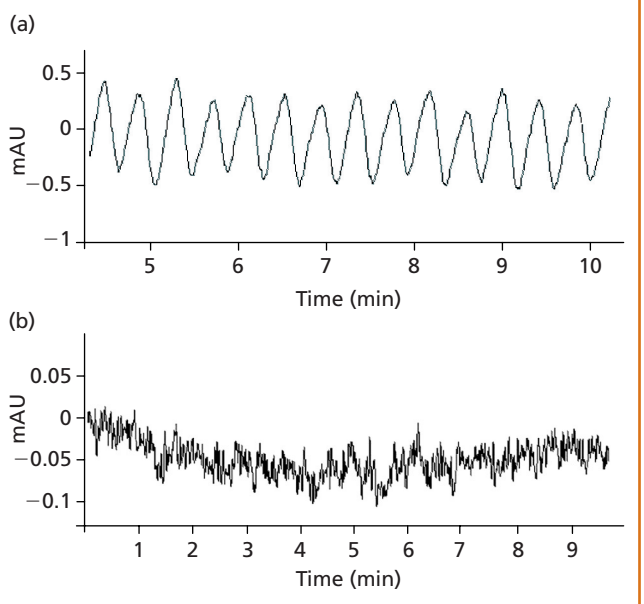

Flow-rate was set at 1.0 mL/min with a pump stroke volume of 20 µL. In the upper trace of Figure 4 a Hypersil 5 µm C18, 125 × 4.0 mm column is used and in the lower trace a restriction capillary, 960 × 0.1 mm, is used instead of this column. Systematic fluctuations, which are seen in the upper trace of Figure 4, have an amplitude approximately 10 times that of the baseline noise, depicted in the lower trace.

The signals do not correlate. However, the systematic fluctuations of the upper trace clearly correlate with the stroke volume delivery time of the B channel (ACN). Peak-to-peak distance averages 25 s. With 1 mL/min at 5% B, the B channel delivers the ACN at 50 µL/min. With a stroke volume of 20 µL, a stroke volume delivery time of 24 s would be expected. In a separate experiment, the composition fluctuations generated by the B pump, were determined as described in the reference manual for the binary pump.[12]

The %B variations were maximally 0.1–0.15% and in most instances were much lower. This means that the particular pump was working well within the specification range. It has also been remarked, that this is usually the situation when the TFA baseline fluctuation problem is reported.

When a linear gradient is applied, the flow-rate of pump B will increase leading to a somewhat more complicated picture, shown in Figure 5. In this Figure, the onset of a linear gradient, 0–100% solvent B in 30 min, is shown. This confirms the observations in Figure 1.

The solvent breakthrough is characterized as a step in the baseline with the systematic fluctuations superimposed on it. With increasing ACN concentration in the mobile phase, the period of the fluctuations and their amplitude decrease. At high ACN concentrations they eventually disappear. Realizing that fluctuations of the ACN concentration in the mobile phase are at the heart of this phenomenon,[2] deliberate introduction of such a mobile phase composition disturbance was investigated. To this end, samples consisting of mobile phase, containing slightly less and slightly more ACN than the mobile phase composition were injected. The results are presented in Figure 6. The upper trace (a) shows a dip followed by a peak, the lower trace (b) reveals the reverse picture.

It is also apparent that this transient type peak response is delayed versus the column dead time. (There are small peaks eluting in front of the transient signal. The first peak is tentatively identified as a dead time marker peak, the second peak as originating from oxygen dissolved in the sample solvent.) It should be noted that, when working with additive-containing eluents, the additive itself can be adsorbed onto the stationary phase and that its affinity for this phase depends on the eluent strength. In this particular instance, it means that the distribution of TFA between the stationary and mobile phase in the column is dependent upon the ACN concentration in the eluent.

In the top trace of Figure 6, at the start of the run, the phase system in the column is in equilibrium with the concentration of TFA in the mobile phase. When the sample is injected, an ACN poor zone, relative to the mobile phase, travels through the column. This zone will tolerate less TFA, so that the TFA is extracted from the mobile phase onto the stationary phase to match the lower ACN concentration in the travelling zone. As the baseline is at a high signal level, because of the absorbance of the TFA, detection of this zone results in a vacancy peak. Once the ACN poor zone has passed, the concentration of TFA on the stationary phase is too high for the solvent composition delivered immediately after the zone and the adsorbed TFA is released into the mobile phase. This results in a positive TFA peak on the baseline.

In the lower trace of Figure 6, the reverse happens. A zone, richer in ACN than the mobile phase, travels through the column resulting first in desorption of TFA into the mobile phase followed by resorption of TFA and a vacancy peak.

Description of the model: As demonstrated above, the baseline disturbances are caused by a change of eluent composition. This causes fluctuations in the background signal of the eluent after the column, even if the concentration of additive in the incoming eluent is maintained. In this section, a model describing this phenomenon is derived for ACN mixtures as

Figure 5: Baseline fragment obtained at the onset of a linear gradient of 0–100% B in 30 min; solvents A and B as in Figure 3; column, detection and flow-rate as in Figure 4.

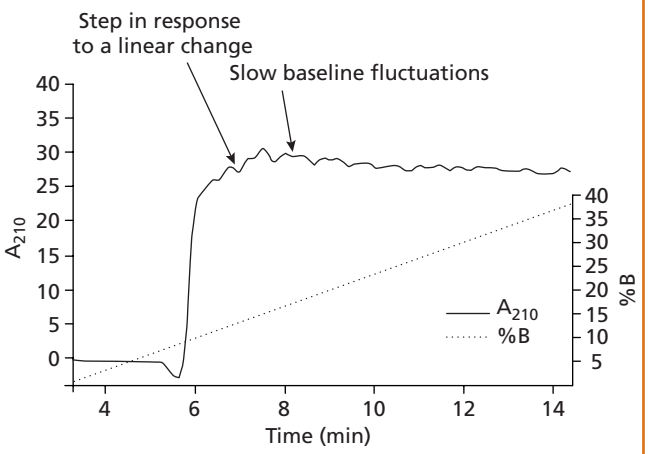

Figure 6: Injection of samples with different solvent compositions in an isocratic mobile phase: 4% ACN in water with 0.1% TFA; (a): sample 5 µL of 3.6% ACN in water with 0.1% TFA; (b): sample 5 µL of 4.4% ACN in water with 0.1% TFA; flow-rate 1 mL/min; column and detection as in Figure 4.

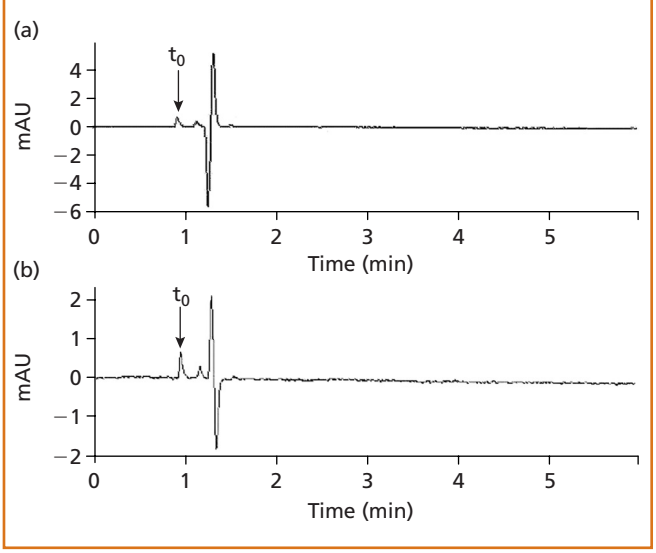

The classic plate theory is a concise example of how to describe the chromatographic process in a quantitative manner. The theory assumes that the solute is at all times in equilibrium with both the mobile and the stationary phase.

eluents with TFA as an additive. In general, the results should be applicable to other phase systems that can be based on this model.[4,5]

The classic plate theory is a concise example of how to describe the chromatographic process in a quantitative manner.[10] The theory assumes that the solute is at all times in equilibrium with both the mobile and the stationary phase. In practice, however, this equilibrium is never achieved because of the continuous progress of the mobile phase through the column. Consequently, the plate theory considers the column to be divided into a number of cells or plates. The size of each cell (the plate height) is such that the solute is considered to have sufficient time to achieve equilibrium in both phases. A smaller cell size corresponds to a more efficient solute exchange between the two phases and will, therefore, result in a higher number of theoretical plates in the given column. The equilibriums within the cells are described by the following equations:

The distribution of a solute between stationary and mobile phase can be represented by:

$$X_s = \alpha X_m \qquad [1]$$

where X_s and X_m are the concentrations of the solute in the stationary and mobile phase, respectively, and α is the distribution coefficient of the solute between the two phases.

Figure 7: Mass transfer steps and redistribution between cells used in the calculation algorithm. The superscript represents the temporal state of a plate and the subscript the serial number of a plate.

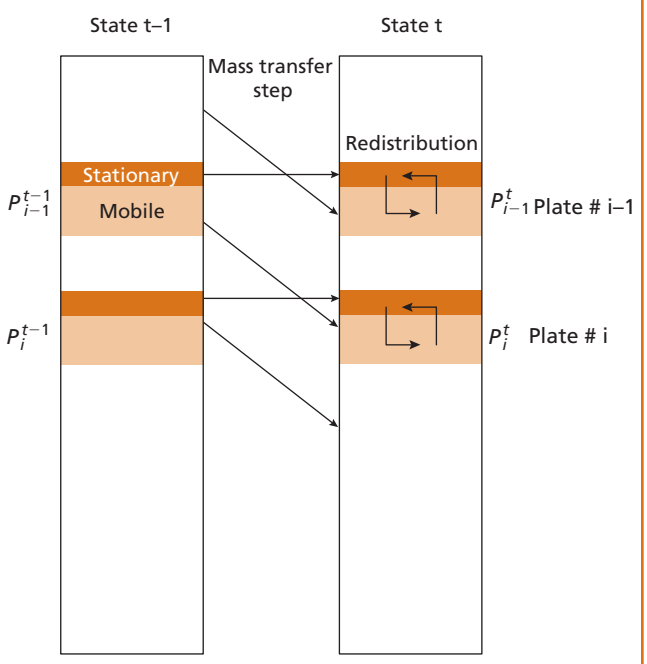

After substituting

$$\frac{m}{V}$$

for X, and the capacity factor, k', for

$$\alpha \frac{V_s}{V_m}$$

one obtains:

$$m_s = k' m_m \qquad [2]$$

For each solute in equilibrium within each cell the conservation of mass is expressed as:

$$m_{total} = m_s + m_m \qquad [3]$$

Combination of Equations 2 and 3 produces:

$$m_m = \frac{m_{total}}{k'+1}, \quad m_s = \frac{m_{total} \cdot k'}{k'+1} \qquad [4]$$

where, within each cell, V_s and V_m are the volumes of stationary and mobile phase; m_s and m_m are the masses of the solute in the stationary and mobile phase and m_{total} is the total mass of the solute.

The elution process is then described by a sequential progress of the portions of mobile phase from one cell to the next with a subsequent redistribution of the solute between both phases of the cell and is depicted in Figure 7.

This process has been computer simulated. Consider a system containing ACN as the strong eluent component and TFA as the additive, and assuming that the changes in the ACN concentration are small, the following approximations can be made:

- The distribution coefficient of ACN between both phases is not affected by minor changes in the ACN concentration.
- The distribution coefficient of TFA is linearly dependent on the ACN concentration within the ACN concentration range (0–10%) considered.
- TFA does not influence the distribution of ACN between both phases.
- The theoretical plate height is the same for both TFA and ACN.

Each mass-transfer step results in replacement of the mobile phase in cell i with that from cell $i-1$. This means that after each mass-transfer step:

$$m_{total_i}^t = m_{m_{i-1}}^{t-1} + m_{s_i}^{t-1} \qquad [5]$$

Combining Equations 4 and 5 for ACN results in Equation 6, which describes the calculation step for ACN:

$$ACN_i^t = \frac{ACN_{i-1}^{t-1}}{k'_{ACN}+1} + \frac{ACN_i^{t-1}.k'_{ACN}}{k'_{ACN}+1} \quad [6]$$

where ACN_i^t represents the mass of ACN at time t in the corresponding cell i.

The equation for TFA is similar to that for ACN with the only difference being that k'_{TFA} is not a constant value but a function of $({}^mACN)$, where $({}^mACN)$ is the ACN concentration in the mobile phase. This leads to:

$$TFA_i^t = \frac{TFA_{i-1}^{t-1}}{k'_{TFA}.({}^mACN_{i-1}^{t-1})+1} + \frac{TFA_i^{t-1}.k'_{TFA}.({}^mACN_i^{t-1})}{k'_{TFA}.({}^mACN_i^{t-1})+1} \quad [7]$$

For the ACN concentration region of simulation (0–10%), a linear dependence of k'_{TFA} with $({}^mACN)$ was assumed:

$$k'_{TFA}({}^mACN_i) = k'_{TFA}(0) - \beta_{TFA}({}^mACN_i) \quad [8]$$

where $k'_{TFA}(0)$ represents the extrapolated k'_{TFA} value in 100% of the weak solvent (water), and β_{TFA} is the slope of the k'_{TFA} versus the ACN concentration plot. Both parameters and also the value for k'_{ACN}, are available from chromatographic measurements and have been determined in separate experiments (details in experimental section).

A chromatographic process can thus be simulated by repeated resolution of Equations 6, 7 and 8 for n cells (n being the plate number) within a column. By changing variables from time (t) to volume (V) the progress of the eluted volume can be simulated and expressed in column volumes ($nV_m + nV_s$), where ($V_m + V_s$) is the volume of a single plate or cell.

Verification of the model: In all experiments and calculations a column of 125 × 4.0 mm packed with 5 µm particles of ODS-Hypersil, able to generate 8000 plates, was used (in some instances a plate number of 1000 has been used to ease calculations, which had minimal influence on the simulation results). The experimentally determined values for k'_{ACN}, $k'_{TFA}(0)$ and β_{TFA} used in the simulations were 0.186, 0.312 and $-0.014(\%\ \mathrm{ACN})^{-1}$, respectively.

In the first example, the injection of non-equilibrated samples (where the solvent composition of the sample differs from the mobile-phase composition) was simulated and depicted in Figure 8.

In the upper part of this figure, a sample zone richer in ACN than the mobile phase was introduced and in the lower part, a sample zone poorer in ACN was applied to the column. The top, red trace in each figure shows the concentration trace for TFA, and the lower, blue trace gives the ACN concentration in the mobile phase. It is clear that the peak for TFA in (a) correlates with the peak for the ACN concentration, while in (b) the dip for TFA correlates with the dip in ACN concentration. The calculated signals are similar to those observed in the experiment depicted in Figure 6. According to theory, the peak areas for the positive TFA peak and its vacancy (dip) should be equal. This was verified in the next experiment, using heptafluorobutyric acid (HFBA) as the mobile phase additive.

Quantitative verification: Heptafluorobutyric acid should be more strongly retained than TFA on the chosen column because of its higher hydrophobicity. As a consequence, k'_{HFBA} should be higher than k'_{TFA}. Applying experimentally determined values for k' of this additive, the model predicts that when a sample of 0.1% HFBA with a higher ACN concentration than the mobile phase is injected, the vacancy peak of HFBA should be more strongly retained than that shown for TFA. Therefore, the differential signal for TFA as shown in Figure 8(a), should be separated for HFBA. In other words, the zone with the higher ACN concentration should be clearly resolved from the retarded negative HFBA peak. This is exactly what is observed in the experiment shown in Figure 9(a).

In this figure, peak 1 is the HFBA peak, and peak 2 is the retained HFBA vacancy peak. The first peak in the trace is again a peak marking the column dead time. The small peak after peak 1 is probably oxygen, dissolved in the sample solvent, which is also shown in Figure 6. Increasing the ACN concentration in the mobile phase can bring the HFBA peak and its vacancy together. This is depicted in Figure 9(b).

Based on the model, it is expected that both HFBA peaks in Figure 9(a) will have the same area. Table 1 shows the experimentally obtained values for the peak areas.

Figure 8: Simulation of the chromatographic process, as illustrated in Figures 6 and 7. Eluent (isocratic): 4% ACN in water with 0.1% TFA; upper trace: 5 µL sample of 4.4% ACN in water with 0.1% TFA; lower trace: 5 µL sample of 3.6% ACN in water with 0.1% TFA.

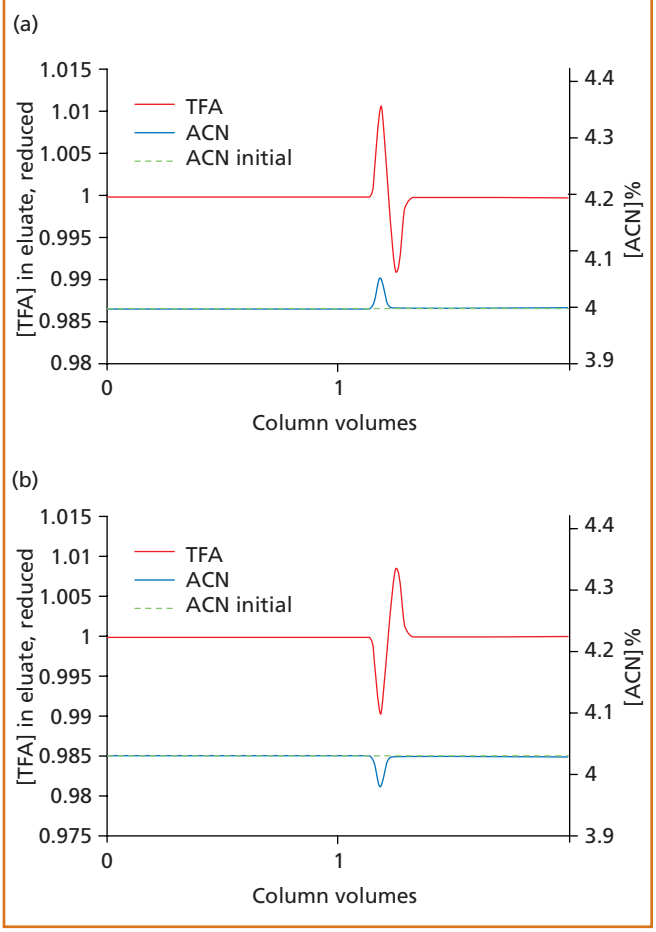

This experiment was simulated, and depicted in Figure 10, by using independently measured values for $k'_{HFBA}(0)$ and β_{HFBA}, which amounted to 2.593 and 0.104, respectively. Again, a good correlation of the simulated pattern and calculated peak areas with the experiment is observed (19.3 mAU.s versus 17.8 mAU.s determined experimentally).

It was then verified whether the model could also predict the signal for a gradient of water/ACN, containing 0.1% TFA, as observed in Figure 5.

As can be seen in Figure 11, the calculated TFA signal indeed predicts the formation of a relatively steep step as a response to a linear change in eluent composition. This is similar to the steps shown in Figures 1 and 5. However, in the actual experiment the fluctuations are superimposed on the step response which are absent in the simulation, because an ideally linear ACN gradient without ACN fluctuations was used in the simulation. The simulated TFA concentration after the step on the gradient onset is 1.038 compared with the initial TFA concentration of 1. The step height (mAU) is thus 0.038 times the signal height corresponding to the initial TFA concentration (0.1%) resulting in 21 mAU. This closely matches the signal height (27 mAU) of the step shown in Figure 5.

We then investigated whether the baseline fluctuations in the TFA signal could be predicted from the deviations of the ACN concentration in the mobile phase.

For one of the pumps a trace pattern of eluent B in the mixture at the column inlet was measured by means of a tracer experiment. A restrictor with the same hydrodynamic resistance replaced the column, and 0.1% acetone was used as a tracer in eluent B. The obtained pattern, which is a composition signal, was used to simulate the TFA signal fluctuations induced by the ACN composition fluctuations given by the tracer signal shown in Figure 12(a).

The simulated TFA signal in Figure 12(a) (lower trace) can be compared with the measured signal for the same pump, and is shown in Figure 12(b). It is evident that the patterns and amplitudes of the irregularities are similar.

Figure 9: (a) Experimental verification of the simulation process with heptafluorobutyric acid (HFBA). Eluent (isocratic): 5% ACN in water with 0.1% HFBA; sample: 5 µL of 6% ACN in water with 0.1% HFBA; column as in Figure 6; detection 214 nm; flow-rate 1 mL/min, and (b) shifts of HFBA system peaks as a function of ACN concentration. Eluents (isocratic): different ACN concentrations in water with 0.1% HFBA; sample: 5 µL of 4% ACN in water with 0.1% HFBA; other conditions as in Figure 9(a).

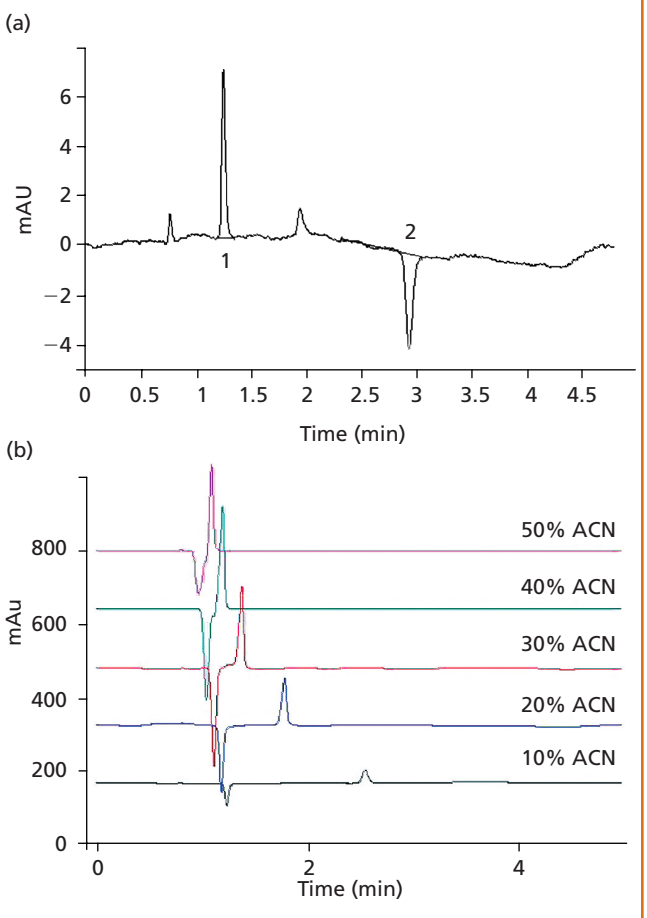

Table 1: Experimental peak areas of peaks 1 and 2 in Figure 9.

Peak	Retention time (min)	Area (mAU seconds)
1	1.274	17.73
2	3.036	17.93

Figure 10: Simulation of the experiment performed in Figure 9(a) under isocratic conditions. Eluent, column, flow-rate and injected sample as in Figure 9(a).

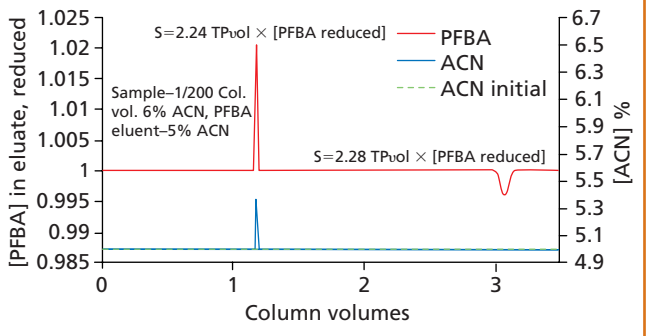

Figure 11: Simulation of the experiment performed in Figure 5 under gradient conditions.

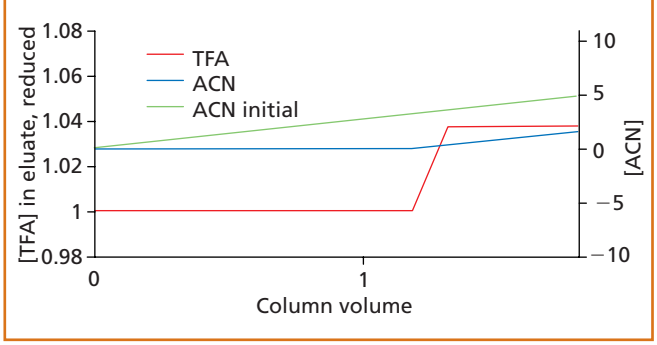

It should be noted that the baseline fluctuations, as shown in Figure 12(b), are caused by composition inconsistencies, which are typical for reciprocating pumps. These fluctuations are maximal for 0.05% B, but they are still 10 times better than the current pump specifications given in the reference manual for the binary pump.[12]

Conclusions

Baseline instabilities with an HPLC system when strongly UV-absorbing mobile-phase additives are used (e.g., 0.1% TFA), have been investigated in a systematic manner. These baseline fluctuations can be explained in a quantitative manner with a plate theory model, which is described and verified in this article.

In essence, the cause of the baseline disturbances is of a general chromatographic nature and will always occur when pumping systems with a measurable level of residual eluent composition fluctuations are used with an UV absorbing additive in the mobile phase that is retained on the stationary phase. The reciprocating pump is certainly able to deliver the solvent composition within the specified range. However, because of the high background absorption of the solvent, a small deviation in the solvent composition will be amplified to a 1–2 mAU baseline fluctuation with a similar width as the peaks to be detected.

Figure 12: (a) ACN profile, reconstructed from a tracer (acetone) measurement at 210 nm (blue), and corresponding simulated A_{210} trace (red) caused by induced TFA fluctuations. Eluent (isocratic): 5% B; solvent A: water; solvent B: 80% ACN in water with 0.1% acetone; restrictor capillary 960 × 0.1 mm; flow-rate 1 mL/min; stroke volume pump B: 20 µL, and (b) experimental A_{210} profile caused by TFA fluctuations using the same pump as in Figure 12(a); detection 210 nm; other conditions as in Figure 12(a).

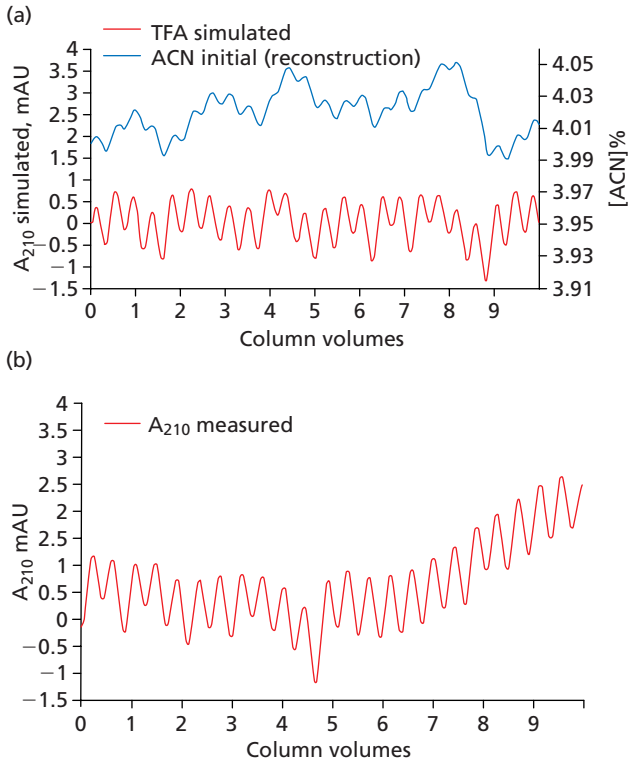

For practical work, the following steps should be taken to reduce the problem:

1. Set the stroke volume of the running channel with as slow a flow-rate as possible.
2. Optimize the compressibility factor settings; especially for the ACN channel.
3. Try to use a TFA concentration of less than 0.1% (v/v).
4. Use leak-tight valves (most important for the active inlet valves).
5. Use an on-line degasser.
6. Add an additional mixer (e.g., the Upchurch solvent filter).
7. Replace TFA with, for example, formic acid, which is less retarded, if the stationary phase used allows (e.g., yields good chromatographic peak shape for tryptic peptides).

Acknowledgements

The authors acknowledge Dr Frank Moffat for providing the chromatogram in Figure 1, Dr Henk Lauer of HLCE, Amsterdam for preparation of the manuscript and fruitful discussions, and Hans-Georg Weissgerber and the Agilent Waldbronn HPLC pump development team for providing support to this work.

References

1. H.P.J. Bennett et al., *Biochem. J.*, **168**, 9–13, (1977).
2. H.E. Schwartz, B.L. Karger and P. Kucera, *Anal. Chem.*, **55**, 1752–1760 (1983).
3. G. Schill and E. Arvidsson, *J. Chromatogr.*, **492**, 299–318 (1989).
4. J.J. Stranahan and S.N. Deming, *Anal. Chem.*, **54**, 1541–1546 (1982).
5. W.E. Barber and P.W. Carr, *J. Chromatogr.*, **316**, 211–225 (1984).
6. S. Levin and E. Grushka, *Anal. Chem.*, **59**, 1157–1164 (1987).
7. J. Crommen et al., *Chromatographia*, **24**, 252–260 (1987).
8. S. Golshan-Shirazi and G. Guiochon, *Anal. Chem.*, **62**, 923–932 (1990).
9. H. Poppe, *J. Chromatogr.*, **506**, 45–60 (1990).
10. R.P.W. Scott, *Liquid Chromatography Column Theory*, R.P.W. Scott and C.F. Simpson, Eds (John Wiley & Sons, Chichester, UK, 1992), 15–19.
11. G. Winkler et al., *J. Chromatogr.*, **347**, 83–88 (1985).
12. Agilent 1100 Series binary pump reference manual, part number: G 1312-90003, edition: 01/00 (Agilent Technologies, Waldbronn, Germany).

Gerard Rozing is a scientific management consultant in the R&D department of Agilent Technologies' LSCA Pharmaceutical Solutions Business Unit in Waldbronn, Germany. Dr Rozing obtained his PhD in organic chemistry at the University of Amsterdam in the Netherlands in 1977 and spent two and a half years as a post-doc in organic chemistry and separation science at the University of Ghent, Belgium and the University of Amsterdam respectively. In 1979 he joined Hewlett-Packard (now Agilent Technologies) in Waldbronn, Germany and has worked as an R&D chemist, group and section manager before occupying his current role.
Konstantin Choikhet obtained his diploma in bioorganic chemistry at the University of Novosibirsk, Russia in 1989 and completed his PhD in separation science at the University of Saarbrücken in Germany in 1995. He joined Agilent Technologies as an R&D chemist in 1999.
Bernd Glatz is an R&D chemist at Agilent Technologies' LSCA Pharmaceutical Solutions Business Unit in Waldbronn, Germany. Dr Glatz obtained his PhD in organic chemistry from the University of Stuttgart, Germany in 1976 and also spent two years there as a post-doc. He has occupied several positions in R&D and marketing at Hewlett-Packard/Agilent Technologies since 1978.